

Nanoscale

Accepted Manuscript



This is an *Accepted Manuscript*, which has been through the Royal Society of Chemistry peer review process and has been accepted for publication.

Accepted Manuscripts are published online shortly after acceptance, before technical editing, formatting and proof reading. Using this free service, authors can make their results available to the community, in citable form, before we publish the edited article. We will replace this *Accepted Manuscript* with the edited and formatted *Advance Article* as soon as it is available.

You can find more information about *Accepted Manuscripts* in the [Information for Authors](#).

Please note that technical editing may introduce minor changes to the text and/or graphics, which may alter content. The journal's standard [Terms & Conditions](#) and the [Ethical guidelines](#) still apply. In no event shall the Royal Society of Chemistry be held responsible for any errors or omissions in this *Accepted Manuscript* or any consequences arising from the use of any information it contains.

**Carboxyl-functionalized polyurethane nanoparticles with
immunosuppressive properties as a new type of anti-inflammatory
platform**

Yen-Jang Huang,^a Kun-Che Hung,^a Fu-Yu Hsieh,^a Shan-hui Hsu^{a,b,*}

^aInstitute of Polymer Science and Engineering, National Taiwan University, Taipei,
Taiwan

^bResearch Center for Developmental Biology and Regenerative Medicine, National
Taiwan University, Taipei, Taiwan

***Shan-hui Hsu (Corresponding author)**

Institute of Polymer Science and Engineering, National Taiwan University, No. 1, Sec.

4 Roosevelt Road, Taipei 10617, Taiwan, R.O.C.

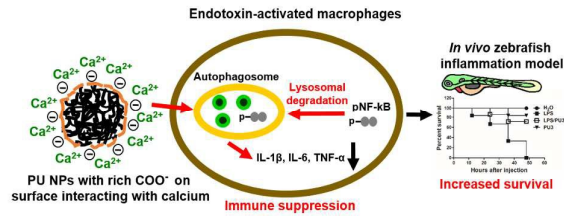
Phone: (886) 2-33665313

Fax: (886) 2-33665237

E-mail: shhsu@ntu.edu.tw

The table of contents:

The novel biodegradable polyurethane nanoparticles display COO^- dependent immunosuppressive properties via autophagy pathway.



Abstract

The interaction of nanoparticles (NPs) with the body immune system is critically important for their biomedical applications. Most NPs stimulate the immune response of macrophages. Here we show that synthetic polyurethane nanoparticles (PU NPs diameter 34–64 nm) with rich surface COO^- functional groups (zeta potential -70 to -50 mV) can suppress the immune responses of macrophages. The specially-designed PU NPs reduces the gene expression levels of proinflammatory cytokines (IL- 1β , IL-6, and TNF- α) for endotoxin-treated macrophages. The PU NPs increase the intracellular calcium of macrophages (4.5–6.5 folds) and activate the autophagy. This is in opposite to the autophagy dysfunction generally observed upon NP exposure. These PU NPs may further decrease the nuclear factor- κB -related inflammation via autophagy pathways. The immunosuppressive activities of PU NPs can prevent animal death by inhibiting the macrophage recruitment and proinflammatory responses, confirmed by an *in vivo* zebrafish model. Therefore, the novel biodegradable PU NPs demonstrate COO^- dependent immunosuppressive properties without carrying any anti-inflammatory agents. This study suggests that NP surface chemistry may regulate the immune responses, which provides a new paradigm for potential applications of NPs in anti-inflammation and immunomodulation.

Introduction

Nanoparticles (NPs) have highly specialized functionality by size, form, and specific surface properties and are widely employed in biological and biomedical applications.¹ Many studies have also indicated that NPs may induce oxidative stress and inflammation to reduce the application efficiency and injure the biological system.^{2,3} Macrophages are critical regulators of innate immune system to eliminate foreign pathogens and to maintain local homeostasis.⁴ They are also involved in many types of chronic inflammatory diseases including atherosclerosis and rheumatoid arthritis, where they play a vital role in the inflammatory process that causes the tissue damage and destruction.^{5,6} Macrophages can sense and remove endogenous and exogenous materials, such as viruses, parasites, cell debris, and foreign particulate materials including a variety of engineered NPs.^{5,7} Cytokines are prime components of innate immunity and inflammation. Particularly, interleukin-1 β (IL-1 β), IL-6, and tumor necrosis factor- α (TNF- α) are involved in the initiation and progression of acute and chronic inflammatory diseases.⁸ Several recent studies have indicated that immune responses of macrophages induced by NPs may be associated with the surface properties of the NPs.^{9,10}

Autophagy is a conserved mechanism that is available for cell growth and homeostasis via degradation of damaged organelles, ubiquitinated proteins, and

pathogens.¹¹ During autophagy, a double membrane structure, the autophagosome, is formed and then merges with the lysosome for breakdown of encapsulated contents. Calcium ion (Ca^{2+}) is a crucial component in autophagy pathways, and the increase of intracellular $[\text{Ca}^{2+}]$ can serve as a potent inducer of autophagy.^{12,13} Cell exposure to NPs can induce cellular autophagy while autophagy dysfunction may play a critical role in NP toxicity.¹⁴ Various kinds of NPs, such as silica NPs, carbon nanotubes, nanoscale titanium dioxide fibers, and amino-functionalized polystyrene NPs may cause lysosomal dysfunction and trigger NP-mediated inflammation.¹⁴ These unwanred immune responses may impede their biomedical applications.

Surface functionalization of NPs not only plays a dominant role in targeting applications but also has great importance on determining the reciprocal interaction between NPs and the surface of biological membranes.⁹ Biodegradable polyurethane (PU) has gained recent attention in biomedical-related fields because of its unique microphase-separated structure, excellent elasticity, and blood compatibility. Using various biodegradable oligodiols for synthesis, PU may have tunable characteristics of degradation time. Moreover, PU has relatively low costs, good mechanical properties, and the surface can be easily modified.^{15,16} These properties facilitate the application of PU NPs as drug nanocarriers, as well as self-assembled platforms for cell culture and tissue engineering.^{17,18} In spite of the critical importance of immunological

properties of NPs on their performance, the immune responses possibly triggered by biodegradable nanomaterials have rarely been investigated so far. In this study, the waterborne PU NPs with distinct surface COO^- contents were examined for their immunomodulatory properties. We expected that macrophages cultured with different PU NPs may show different extents of immune responses through autophagy activation. To our surprise, we observed that these functionalized PU NPs could suppress the immune response of macrophages instead of provoking it. The engineered PU NPs with particular surface modifications may serve as a platform to understand how the surface chemistry of NPs regulates immune responses and to explore NPs as potential new anti-inflammatory agents.

2. Experimental section

Synthesis and characterization of waterborne PU NPs

PU NPs were synthesized via an aqueous process.¹⁹ PCL diol ($M_n \sim 2$ kDa, Sigma) was used as the soft segment to react with IPDI (Evonik Degussa GmbH) under nitrogen for 3 h at 75°C. The ionic chain extender DMPA (Sigma) and methyl ethyl ketone (13 mL) (MEK, J.T. Baker) were then added to react for 1 h after the prepolymerization. When the temperature was decreased to 45°C, triethylamine (TEA, RDH) was used to neutralize the carboxylic group of DMPA for 30 min. The

neutralized prepolymer was then dispersed in deionized water by vigorous stirring. Finally, a second chain extender EDA (Tedia) was added to react for another 30 min. The residual MEK and TEA was removed by vacuum distillation. The final product was PU NPs suspended in distilled water. The solid content of the aqueous dispersion was about 30 wt% PU NPs. There were three types of PU NPs with different ionic contents where DMPA ratios were 4.0, 4.2, and 4.4 wt% with respect to the whole PU molecule. PUs containing 4.0%, 4.2%, and 4.4% DMPA were each abbreviated as PU1, PU2, and PU3. The stoichiometric ratios of IPDI/PCL diol/DMPA/EDA for each type of PU NPs were 3.47/1/0.95/1.52 (PU1), 3.52/1/1/1.52 (PU2), and 3.57/1/1.05/1.52 (PU3). For the synthesis of amine-rich PU NPs (PU-N), N-methyldiethanolamine (N-MDEA, Acros) that carries positive amine group was used to replace DMPA that carries COO^- group. The hydrodynamic diameter of PU NPs was determined by dynamic light scattering and the zeta potential was measured by electrophoretic light scattering, using a submicron particle analyzer (Delsa Nano, Beckman Coulter, USA).

Cell culture

J774A.1 macrophage cells were grown in continuous culture in Dulbecco's modified Eagle's medium (DMEM) (Gibco) supplemented with 10% fetal bovine serum (FBS)

(Gibco) and 1% penicillin–streptomycin–amphotericin (PSA) (Gibco). Cells were maintained in a humidified incubator at 37°C and 5% CO₂, and subcultured twice per week. Cells (2.5×10^5) were seeded in 6-well culture plates and the morphology was observed by an inverted microscope (Leica, DMIRB).

Cell viability assay

J774.A1 cells were seeded at 1×10^4 cells/well in 96-well plates in the complete medium at 37°C. After 24h, cells was treated PU NPs for 30 min, and then incubated with lipopolysaccharide (LPS) (sigma) for 24 h. Cell viability was measured by WST-1 assay (Roche).The absorbance was measured at 450 nm using a microplate reader (SpectraMax® M5, USA).

Quantitative real time reverse transcription-polymerase chain reaction (qRT-PCR) analysis

The mRNA expression for proinflammatory cytokines and autophagy-related gene was analyzed by qRT-PCR. Trizol® reagent (Invitrogen) was used to extract total RNA from cells according to manufacturer's instruction. Total RNA (1 µg) was reverse-transcribed into cDNA by the RevertAid First Strand cDNA Synthesis Kit (MBI Fermentas, St. Leon-Rot, Germany). QRT-PCR was conducted in a Chromo 4

PTC200 Thermal Cycler (MJ Research, USA) using the DyNAmo Flash SYBR Green qPCR Kit (Finnzymes Oy, Espoo, Finland). QRT-PCRs were performed using primers for interleukin 1 beta (IL-1 β), interleukin 6 (IL-6), tumor necrosis factor (TNF- α), autophagy related 5 (ATG5), beclin 1, cathelicidin, mechanistic target of rapamycin (Mtor), and glyceraldehyde 3-phosphate dehydrogenase (GAPDH). The gene expression levels were normalized to those of GAPDH. The normalized value was then shown as the relative ratio to that in the mock group. The primer sequences are listed in Table 1.

Western blot analysis

J774.A1 cells were seeded at a density of 2.5×10^5 cells per well in a 6-well culture plate and cultured for 24 h. Cells were incubated with PU NPs for 30 min and then were treated with LPS. After 24 h treatment, cells were harvested and lysed in lysis buffer containing 20 mM HEPES (pH 7.5), 420 mM NaCl, 1.5 mM MgCl₂, 0.1% NP-40, and protease inhibitor cocktail (Sigma). Sample proteins were separated by 15% sodium dodecyl sulfate polyacrylamide gel electrophoresis (SDS-PAGE) and then transferred to a nitrocellulose membrane. Proteins were bound to rabbit polyclonal anti-LC3 antibody (Genetex), rabbit monoclonal anti-p-NF- κ B (Genetex), and rabbit monoclonal anti-GAPDH antibody (Genetex). The intensities of protein

bands were detected by Labwork software (UVP). The related protein expression was quantified by the software ImageJ.

Calcium-binding capacity of PU NPs

PU NPs were placed in DMEM medium without FBS at 37°C for 24 h. Samples were centrifuged at 6000 rpm for 20 min at 25°C by Amicon Ultra-4 centrifugal filter devices (Millipore). Samples from the button of Amicon Ultra tubes were collected for analysis of the calcium content remained in the solution. The concentration of calcium in the medium was measured by the atomic absorption spectrometry (AA, iCE 3300; Thermo Scientific, USA). The amount of PU NP-bound calcium was calculated by subtracting the content of calcium in the collected solution from those in DMEM medium. The medium without PU NP incubation was used as the control. PU NPs from the upper side of Amicon Ultra tubes were collected and washed three times by H₂O in Amicon Ultra-4 centrifugal filter devices (Millipore). The PU films were made by PU NP dispersion on 15 mm microscope coverslip glass at 25°C. The surface functional groups of the PU films were evaluated by the attenuated total reflection-Fourier transform infrared spectroscopy (ATR-IR, Spectrum 100, Perkin-Elmer, USA).

Immunocytochemistry

After LPS and PU NP treatment, J774.A1 cells were washed with PBS and fixed in 4% paraformaldehyde at room temperature for 10 min. Cells were washed with 1% Tween/PBS and incubated with rabbit polyclonal anti-LC3 antibody (Genetex) for autophagosomes and rabbit monoclonal anti-p-NF- κ B antibody (Genetex) for NF- κ B activation. The second antibodies were goat anti-rabbit IgG (FITC) (Santa cruz) for LC3 and Donkey anti-rabbit IgG (Alexa Fluor 594) (Biolegend). Cells were analyzed using a fluorescence microscope.

LPS-induced zebrafish inflammation model

AB (wild type) zebrafish embryos were purchased from the Zebrafish International Resource Center (Oregon, USA) and were raised, maintained, and paired under standard conditions. Zebrafish embryos were incubated in a petri dish with the E3 embryo medium (5 mM NaCl, 0.17 mM KCl, 0.33 mM CaCl₂, and 0.33 mM MgSO₄) at 28°C. The embryos were staged according to the number of somites, hours post fertilization (hpf), and days post fertilization.²⁰ Zebrafish embryos were divided into four groups in this study. The blank control group was H₂O was injected into yolk of zebrafish embryos at 48 hours hpf. The experimental groups were inject with LPS (1.25 ng), PU3 (500 pg), or LPS/PU3 co-injected. Each group of embryos was then

cultured at 28°C and observed for signs of inflammatory responses by neutral red staining. Neutral red accumulates in the lysosomes through endocytosis. As macrophage cells undergo efficient endocytosis, NR labels macrophages more stable than any other cell types. Optimal staining of macrophages in live embryos was achieved by incubating embryos in 2.5 µg/mL NR solution containing 0.003% PTU at 28°C in the dark for 6–8 h.²¹ After staining, macrophages were observed using a Leica (Z16 APO) stereomicroscope. All tests were performed on multiple samples (n= 30) and repeated by three independent experiments. All procedures involving zebrafish work in this study followed the ethical guidelines and were approved by the Institutional Animal Care and Use Committee (IACUC).

Statistical analysis

Data from multiple samples were expressed as the mean ± standard deviation. Three similar experiments at least were performed independently for each type of experiment. Typical data were shown in this study. Statistical differences among the experimental groups were evaluated by one way ANOVA. The survival rate was analysed using the Kaplan-Meier survival curve and log-rank test. *p*-Values <0.05 were considered statistically significant.

Results and discussion

Synthesis and Characterization of PU NPs

The detailed synthesis procedure of waterborne PU NPs was described in a previous study with modification of stoichiometry in the current study.¹⁹ The structure of PU NPs consisted of about 66% (weight) soft segment [poly(ϵ -caprolactone) diol (PCL diol)] and 34% hard segment [isophorone diisocyanate (IPDI), 2,2-bis(hydroxymethyl) propionic acid (DMPA), and ethylenediamine (EDA)] linked by urethane and urea bonds. Various PU NPs prepared in this study are illustrated in Fig. 1a. The ionic component DMPA contained $-\text{COOH}$ groups and accounted for 4.0, 4.2, and 4.4% of the PU NP weight for PU1, PU2, and PU3, respectively, confirmed by NMR. The synthesis yielded the stable aqueous dispersion of PU NPs (about 30% solid content). The content (concentration) of PU NPs could be easily adjusted from the stock dispersion. The diameter and zeta potential of the various PU NPs were determined by light scattering. The NPs of PU1 had a hydrodynamic diameter of 64.3 ± 0.8 nm and a zeta potential of -48.1 ± 3.9 mV. The NPs of PU2 had a smaller hydrodynamic diameter (41.9 ± 0.7 nm) and a more negative zeta potential (-63.1 ± 3.5 mV). The NPs of PU3 had the smallest hydrodynamic diameters (34.0 ± 1.3 nm) and the most negative zeta potential (-70.8 ± 0.8 mV) (Table 2). The surface chemistry was defined by attenuated total reflectance-Fourier transform infrared spectroscopy (ATR-FTIR).

The IR absorption peaks at 1730 cm^{-1} and 1670 cm^{-1} indicated free and bound carbonyl groups (C=O) in the PU structure, respectively.²² The peak at 2865 cm^{-1} was attributed to the CH_2 stretching vibrations (Fig. 1b). The values of total (free and bound) C=O versus CH_2 observed in PU3 was greater than that in PU1 and PU2 (Fig. 1c). Based on the changes in ATR-IR absorption as well as the values of zeta potential, PU3 had higher surface carboxyl-modification than PU1 and PU2.

Immune Suppression of Macrophages by PU NPs

The effect of PU NPs on the immune responses of J774.A1 macrophage mouse cell line was assessed after incubation with different PU NPs. The normal morphology of macrophages cells was in round shape. After treatment with different types of PU NPs, the morphology of macrophages remained relatively normal. The intracellular PU NPs were clearly observed for cells treated with PU NPs at the concentration of $50\text{ }\mu\text{g/ml}$ (Fig. 2a). The mRNA expressions of proinflammatory genes were obviously upregulated after endotoxin (lipopolysaccharide, LPS) treatment. In the PU NP-treated groups, the expression levels of all these genes were not higher than the mock group (Fig. 2b). To examine the cytotoxicity of PU NPs, we treated macrophages with different concentrations of PU NPs. No significant effect on cell

viability was observed at 24 h in any group (Fig. 2c). These results indicated that PU NPs themselves did not cause any immune stimulation.

To further evaluate the immune regulation of PU NPs, we treated macrophages with LPS and PU NPs. After treatment with LPS, the macrophages showed a spread shape. However, the macrophages still kept relatively round morphology in all LPS/PU NP groups (Fig. 3a). PU NPs at a lower dose (10 $\mu\text{g/ml}$) significantly reduced the LPS-induced enhancement in IL-1 β , IL-6, and TNF- α mRNA expressions, but there was no obvious difference of immunosuppressive activities among the three PU NP groups. The inhibition of proinflammatory genes was even more remarkable at higher dose (50 $\mu\text{g/ml}$) of PU NPs. Among the three PU NP groups, PU3 exhibited greater capacities of inhibiting the proinflammation genes than PU1 and PU2 under LPS stimulation, but the immunosuppressive activities by PU1 and PU2 was not statistically different. (Fig. 3b). In general, PU NPs showed immunosuppressive activities on macrophages. Particularly, PU NPs with more surface carboxyl groups (PU3) showed greater immune suppression effects.

The Calcium Binding Capacity of PU NPs

We then studied how the difference in surface negative charge of PU NPs affected the calcium adsorption. We mixed PU NPs with culture medium, and then isolated PU

NPs for quantitative measurements of calcium by atomic absorption spectroscopy. After removing PU NPs, the calcium concentration of culture medium was reduced in all PU NP groups. The amount of calcium adsorbed on PU NPs was calculated based on the reduced concentration of calcium in the medium. The NPs of PU3 showed more calcium binding capacity than those of PU1 and PU2 (Fig. 4a). To track the surface-bound calcium of PU NPs, we incubated PU NPs with Calcium Green-1, AM so the surface-bound calcium was labeled with fluorescence before contacting with cells. The fluorescent images revealed that the NP-bound calcium was later transported into macrophages after exposure to PU NPs (Fig. 4b). We further determined the fluorescent calcium positive cells by flow cytometry. The fluorescence intensity of intracellular pre-labeled calcium showed that the NPs of PU3 tended to move a greater amount of calcium into cells (Fig. 4c). The surface bound calcium was chemically characterized by the ATR-FTIR spectra (Fig. 4d). The IR absorption peak at 1730 cm^{-1} is associated with the stretching vibration of carbonyl groups (C=O) in the PU structure. This peak was shifted to a lower wavenumber (1721 cm^{-1}) after incubation with the culture medium. The shift of this peak suggested the binding of COO^- with calcium.

Induction of Autophagy by PU NPs

Since calcium entry may induce cell autophagy, we examined whether PU NPs induced macrophage autophagy. For the purpose, the endogenous expression of an autophagosomal marker, LC3-II, was detected by Western blots. It was found that the LC3-II protein expression increased after incubation with PU NPs. Among the NPs, PU3 induced a greater level of LC3-II expression than PU1 and PU2 (Fig. 5a). The LC3-II protein expression was also slightly increased in the group of LPS treatment (1.4-folds). For the combined treatment of LPS and PU3, the LC3-II expression was increased by a notable 3.4-fold, which also resulted in obvious LC3 puncta compared to the group treated with LPS or PU3 alone (Fig. 5b and c). The autophagy component genes [autophagy related 5 (ATG5), beclin 1, and cathelicidin] as well as the autophagy inhibition gene mechanistic target of rapamycin (Mtor) were further examined. Results showed that ATG5, beclin 1, and cathelicidin genes were all upregulated in the LPS/PU3 group. However, the mRNA expression of Mtor had no difference among the groups (Fig. 5d). The cell viability remained unchanged after treatment of LPS and PU3 (Fig. 5e).

Regulation of NF- κ B Pathway via PU NP Triggered Autophagy

To identify the possible role of autophagy in regulating NF- κ B pathway, the localization of LC3 and phospho-NF- κ B p65 (p-NF- κ B) were examined by the

fluorescence microscopy. Macrophages showed more autophagosome formation and stronger immunofluorescence staining in the LPS/PU3 group, while exhibited a weak and diffuse cytoplasmic staining in the other groups. Furthermore, macrophages showed clear autophagosomes and p-NF- κ B colocalization in the LPS/PU3 group (Fig. 6a). Moreover, the LPS-induced p-NF- κ B activation was also inhibited in the LPS/PU3 group (Fig. 6b). When macrophages were incubated with EGTA (a Ca²⁺ chelator) or Bafilomycin A1 (Baf-A1, a lysosomal inhibitor) in the LPS/PU3 group, the expression of LC3-II protein was attenuated (Fig. 6c). Furthermore, the mRNA gene expression levels of IL-1 β , IL-6, and TNF- α were also recovered by the treatment of EGTA or Baf-A1 in the LPS/PU3 group (Fig. 6d). These data suggested that PU3 may reduce the NF- κ B-related inflammation via autophagy pathways.

In Vivo Anti-Inflammatory Activity of PU NPs in the LPS-Induced Zebrafish Inflammation Model

LPS can induce acute inflammatory responses of zebrafish embryos by the recruitment of macrophage to the yolk and upregulation of proinflammatory cytokines.²¹ As demonstrated by the neutral red (NR) staining, macrophages were significantly recruited to the injection site (indicated by arrows) after LPS injection compared with H₂O-injected control. The co-treatment with PU3 greatly reduced such

recruitment (Fig. 7a). Analyses of the LPS-injected embryos showed remarkable increases in the mRNA expression of proinflammatory cytokines (IL-1 β , IL-6, and TNF- α) by 14-, 37-, and 3.6-folds, respectively. The levels of these proinflammatory cytokines were significantly decreased by PU3 co-injection (Fig. 7b). Moreover, LPS injection alone caused 100% mortality of the experimental animals within 48 hours post injection (hpi). In contrast, the PU3 co-treatment reduced the mortality to 29% (Fig. 7c). These *in vivo* results further supported that PU NPs displayed potential immunosuppression against endotoxin-induced inflammation.

Nanomedicine has a great potential to change the way of diagnosis and therapy for many diseases. The immune responses triggered by nanomedicine are harmful but can also be useful (e.g. in cancer therapy).⁷ Water-based PU NPs have potential biomedical applications.^{16,19} However, the immune responses of PU NPs or any other biodegradable polymer NPs remain poorly understood, particularly at the molecular level. When NPs enter the body, macrophages rapidly perceive and take up NPs through phagocytosis, micropinocytosis, and various endocytotic pathways.²³ In most cases, NP exposure in macrophages leads to proinflammatory responses and cell death.²⁴ In contrast, we demonstrated in this study that direct exposure of macrophages to PU NPs reduced proinflammatory cytokine production and led to immune suppression through activation of autophagy and the subsequent dysfunction

of the NF- κ B (inflammation) pathways. Moreover, PU NPs could reduce the inflammation-related animal mortality by inhibiting the macrophage recruitment and proinflammatory cytokines in the *in vivo* zebrafish inflammation model (Fig. 8).

The surface modification of NPs is an important issue for designing suitable cell-targeting and drug-carrier nanomaterial systems.²⁵ Studies showed that surface modification of NPs with amino groups, but not carboxyl groups, could directly induce inflammation and inhibit proliferation in immune cells.^{9,10} The amino-functionalized polystyrene NPs had immunostimulatory properties by triggering the lysosomal destabilization in macrophages, whereas the carboxyl- or nonfunctionalized polystyrene NPs “did not induce any immune response.”⁹ In the present study, we observed that PU NPs were internalized and accumulated in the macrophages. Besides, PU NPs did not directly influence cell morphology or viability. Meanwhile, the gene expressions of the proinflammatory cytokines were reduced with PU NP treatment. These data suggested that PU NPs did not cause serious immune stimulating properties or cytotoxicity in macrophages. Excessive production of proinflammatory cytokines, such as IL-1 β , IL-6 and TNF- α , contributes to harmful inflammatory reactions of most NPs. Strikingly, we observed that carboxyl-modified PU NPs dramatically reduced the response of macrophages to LPS by downregulating the gene expressions of IL-1 β , IL-6, and TNF- α . In contrast, the phenomena did not

occur in surface amine-modified PU NPs (PU-N, hydrodynamic diameter 105 ± 5.6 nm, zeta potential 58.7 ± 0.8 mV). The macrophages remained the spread shape and the gene expressions of IL-1 β , IL-6, and TNF- α were not significantly reduced after LPS/PU-N treatment (Supporting information, Fig. S1a and b). These findings suggest a robust anti-proinflammatory response after certain functionalized PU NP treatment.

In this study, we designed PU NPs with different amounts of functionalized carboxyl groups on the surface of NPs and showed that they were able to bind calcium in different extents. We hypothesized that the hydrophilic segments (such as COO⁻, C=O, C-N) of the PU NPs may adsorb calcium ion through coordination and the cage effect.^{26,27} PU NPs may thus transport Ca²⁺ from the extracellular environment into macrophages. The flow cytometry confirmed the increases in intracellular calcium and dependency upon on the amount of carboxyl groups on PU NPs. Because calcium influx was reported to promote autophagy activation^{28,29}, PU NPs with rich surface carboxyl groups may have a potential to induce autophagy activation.

The process of autophagy has generally been regarded as a pro-survival mechanism, whereas excessive levels of cellular autophagy can result in cell death.³⁰ A recent investigation revealed that many NPs provoked cytotoxicity by inducing

autophagy dysfunction.^{14,31} Although macrophages exhibited a high level of autophagy activation after LPS and PU NPs co-treatment, the cell viability remained unaffected. Autophagy has unveiled its roles in innate immunity by clearing the apoptotic cells as a potential mechanism to control inflammation.³² Therefore, we suggested that the PU NP-mediated autophagy increase may limit the NF- κ B activities of macrophages after endotoxin-induced inflammation. A normal autophagosome fuses with a lysosome to degrade the encapsulated content, while in this study we observed the colocalization of p-NF- κ B and autophagosome. Besides, the immune suppression by PU NPs was attenuated after treatment with the autophagy inhibitors EGTA and Baf-A1. In another words, PU NPs may reduce NF- κ B dependent immune response by the autophagy-lysosome pathway. According to literature, autophagy is important for the macrophage survival and can be activated during the differentiation of macrophages.³³ IL-1 β , IL-6 and TNF- α are major cytokines secreted by M1-type macrophages but autophagy regulates NF- κ B lysosomal degradation in M2-type macrophages.^{34,35} Since PU NPs also inhibited the proinflammatory cytokines and reduced the NF- κ B activation, the possible roles of PU NPs in macrophage differentiation may worth further investigation.

Zebrafish has been emerged recently as an excellent model for studying the pathophysiology of human immune-related diseases. The large number of progeny

greatly facilitates genetic analysis. Moreover, the embryo is transparent to allow fluorescent tracking of labeled cells. These advantages make the zebrafish model suitable for high-throughput *in vivo* drug screening and NP studies. In this study, the endotoxin-induced zebrafish inflammation model was used to confirm the immunosuppressive activities of PU NPs *in vivo*. The treatment inhibited the macrophage recruitment and proinflammatory responses, and particularly, reduced the animal death. The injection by PU NPs alone could slightly increase the expression of TNF- α , but not IL-1 β and IL-6, and it did not cause significant macrophage accumulation or mortality compared with the H₂O-injected control. Since NPs can deliver conventional drugs, proteins, and nucleotides, we believe that PU NPs may be further designed to bind immunosuppressive agents to promote their therapeutic effects on human immune-related diseases.

Dysfunction of autophagy involves in the progression of degenerative changes in mammalian tissues, like pathological aging and neurodegenerative diseases. Induction of autophagy has proved to be a useful mechanism for therapeutic applications.^{36,37} The exposure to engineered nanomaterials may regulate the responses of biological systems and have received growing attention. In contrast to the autophagy dysfunction recently reported for many NPs¹⁴, the current PU NPs induced strong autophagy activation without toxicity. This property of PU NPs may be applied not only in

anti-inflammation, but also potentially in aging and neurodegeneration related diseases. Finally, because the current PU NPs are biodegradable organic NPs with rich surface functional groups, they may be conveniently engineered as drug carriers to further improve therapeutic effects in diseases.

Conclusions

Carboxyl-functionalized PU NPs can induce autophagy activation and immune suppression in macrophages through increasing intracellular calcium. PU NPs with more surface carboxyl groups induce more calcium entry and show stronger immune suppressive activities. The autophagy associated with PU NP uptake further blocks inflammatory NF- κ B activation by protein degradation in autophagosomes. Therefore, surface modification with carboxyl groups may turn biologically inert organic nanoparticles into potent inhibitors of inflammatory responses. The surface chemistry of NPs determines their immune regulatory effects and may be designed for potential new applications in anti-inflammation and immunomodulation

Acknowledgements

This research was supported by the Aim for the Top University Plan (103R4000) of Ministry of Education and the Ministry of Science and Technology

(MOST103-2321-B-002-100), Taiwan, R.O.C. We thank the Taiwan Zebrafish Core Facility at National Taiwan University (NTU-ERP-104R8600) for the facility and technical supports.

References

1. R. Subbiah, M. Veerapandian and K. S. Yun, *Curr. Med. Chem.*, 2010, **17**, 4559-4577.
2. C. Guo, Y. Xia, P. Niu, L. Jiang, J. Duan, Y. Yu, X. Zhou, Y. Li and Z. Sun, *Int. J. Nanomedicine.*, 2015, **10**, 1463-1477.
3. N. Li, T. Xia and A. E. Nel, *Free Radic. Biol. Med.*, 2008, **44**, 1689-1699.
4. B. Opitz, V. van Laak, J. Eitel and N. Suttorp, *Am. J. Respir. Crit. Care Med.*, 2010, **181**, 1294-1309.
5. F. Chellat, Y. Merhi, A. Moreau and L. Yahia, *Biomaterials.*, 2005, **26**, 7260-7275.
6. S. Amor, L. A. Peferoen, D. Y. Vogel, M. Breur, P. van der Valk, D. Baker and J. M. van Noort, *Immunology.*, 2014, **142**, 151-166.
7. H. J. Yen, S. H. Hsu and C. L. Tsai, *Small.*, 2009, **5**, 1553-1561.
8. T. H. Mogensen, *Clin. Microbiol. Rev.*, 2009, **22**, 240-273.
9. O. Lunov, T. Syrovets, C. Loos, G. U. Nienhaus, V. Mailander, K. Landfester, M. Rouis and T. Simmet, *ACS nano.*, 2011, **5**, 9648-9657.

10. C. Loos, T. Syrovets, A. Musyanovych, V. Mailander, K. Landfester and T. Simmet, *Biomaterials.*, 2014, **35**, 1944-1953.
11. M. Komatsu and Y. Ichimura, *Genes Cells.*, 2010, **15**, 923-933.
12. M. Hoyer-Hansen, L. Bastholm, P. Szyniarowski, M. Campanella, G. Szabadkai, T. Farkas, K. Bianchi, N. Fehrenbacher, F. Elling, R. Rizzuto, I. S. Mathiasen and M. Jaattela, *Mol. Cell.*, 2007, **25**, 193-205.
13. J. P. Decuypere, D. Kindt, T. Luyten, K. Welkenhuyzen, L. Missiaen, H. De Smedt, G. Bultynck and J. B. Parys, *PloS one.*, 2013, **8**, e61020.
14. S. T. Stern, P. P. Adisheshaiah and R. M. Crist, *Part. Fibre. Toxicol.*, 2012, **9**, 20.
15. D. Tan, L. Liu, Z. Li and Q. Fu, *J. Biomed. Mater. Res. A.*, 2015, **103**, 2711-2719.
16. K. C. Hung, C. S. Tseng and S. H. Hsu, *Adv. Healthc. Mater.*, 2014, **3**, 1578-1587.
17. Y. C. Kuo, S. C. Hung and S. H. Hsu, *Colloids Surf. B Biointerfaces.*, 2014, **122**, 414-422.
18. M. C. Tsai, K. C. Hung, S. C. Hung and S. H. Hsu, *Colloids Surf. B Biointerfaces.*, 2015, **125**, 34-44.
19. S. H. Hsu, K. C. Hung, Y. Y. Lin, C. H. Su, H. Y. Yeh, U. S. Jeng, C. Y. Lu, S. H. A. Dai, W. E. Fu and J. C. Lin, *J. Mater. Chem. B.*, 2014, **2**, 5083-5092.

20. C. B. Kimmel, W. W. Ballard, S. R. Kimmel, B. Ullmann and T. F. Schilling, *Dev. Dyn.*, 1995, **203**, 253-310.
21. L. L. Yang, G. Q. Wang, L. M. Yang, Z. B. Huang, W. Q. Zhang and L. Z. Yu, *Molecules.*, 2014, **19**, 2390-2409.
22. X. Jiang, J. H. Li, M. M. Ding, H. Tan, Q. Y. Ling, Y. P. Zhong and Q. Fu, *Eur. Polym. J.*, 2007, **43**, 1838-1846.
23. D. A. Kuhn, D. Vanhecke, B. Michen, F. Blank, P. Gehr, A. Petri-Fink and B. Rothen-Rutishauser, *Beilstein J. Nanotechnol.*, 2014, **5**, 1625-1636.
24. S. K. Sohaebuddin, P. T. Thevenot, D. Baker, J. W. Eaton and L. Tang, *Part. Fibre. Toxicol.*, 2010, **7**, 22.
25. W. H. De Jong and P. J. Borm, *Int. J. Nanomedicine.*, 2008, **3**, 133-149.
26. D. N. Kalu, B. C. Miyasaki and G. V. Foster, *Calcif. Tissue Res.*, 1974, **16**, 1-12.
27. D. E. Clapham, *Cell.*, 2007, **131**, 1047-58.
28. X. Chen, M. Li, D. Chen, W. Gao, J. L. Guan, M. Komatsu and X. M. Yin, *PLoS one*, 2012, **7**, e52347.
29. S. S. Smaili, G. J. Pereira, M. M. Costa, K. K. Rocha, L. Rodrigues, L. G. do Carmo, H. Hirata and Y. T. Hsu, *Curr. Mol. Med.*, 2013, **13**, 252-265.
30. Y. Tsujimoto and S. Shimizu, *Cell Death. Differ.*, 2005, **12 Suppl 2**, 1528-1534.
31. H. W. Chiu, T. Xia, Y. H. Lee, C. W. Chen, J. C. Tsai and Y. J. Wang, *Nanoscale.*,

- 2015, **7**, 736-746
32. P. Kuballa, W. M. Nolte, A. B. Castoreno and R. J. Xavier, *Annu. Rev. Immunol.*, 2012, **30**, 611-646.
33. Y. Zhang, M. J. Morgan, K. Chen, S. Choksi and Z. G. Liu, *Blood.*, 2012, **119**, 2895-2905.
34. J. W. Tjiu, J. S. Chen, C. T. Shun, S. J. Lin, Y. H. Liao, C. Y. Chu, T. F. Tsai, H. C. Chiu, Y. S. Dai, H. Inoue, P. C. Yang, M. L. Kuo and S. H. Jee, *J. Invest. Dermatol.*, 2009, **129**, 1016-1025.
35. C. P. Chang, Y. C. Su, C. W. Hu and H. Y. Lei, *Cell Death. Differ.*, 2013, **20**, 515-523.
36. D. C. Rubinsztein, G. Marino and G. Kroemer, *Cell.*, 2011, **146**, 682-695.
37. W. E. Hochfeld, S. Lee and D. C. Rubinsztein, *Acta Pharmacol. Sin.*, 2013, **34**, 600-604.

Figure captions

Fig. 1 (a) The chemical structure and synthetic process of PU NPs with different DMPA contents in compositions (PU1, PU2, and PU3). (b) The IR spectra of PU with different COO^- contents. (c) The relative absorption values of the functional groups expressed as the semi-quantitative ratios of total (free and bound) $\text{C}=\text{O}$ versus CH_2 .

Fig. 2 (a) The morphologies of macrophages after incubation with PU NPs (50 $\mu\text{g}/\text{ml}$) for 24 h. Scale bar represents 100 μm . (b) The mRNA expressions of proinflammatory cytokine genes after incubation of PU NPs (10 or 50 $\mu\text{g}/\text{ml}$) for 24 h. Endotoxin (LPS) served as the positive control. (c) The viability of macrophages after treatment of of PU NPs at various concentrations (1.5~200 $\mu\text{g}/\text{ml}$) for 24 h. ns, no significant difference.

Fig. 3 (a) The morphologies of macrophages after incubation with PU NPs (50 $\mu\text{g}/\text{ml}$) for 30 min and then treated with LPS (100 ng/ml) for 24 h. Scale bar represents 100 μm . (b) The mRNA expressions of proinflammatory cytokine genes for macrophages after incubation with PU NPs (10 or 50 $\mu\text{g}/\text{ml}$) for 30 min and then treatment with LPS (100 ng/ml) for 24 h. $*p < 0.05$, among the indicated groups.

Fig. 4 (a) The amount of calcium bound by PU NPs in DMEM medium after placing PU NPs (50 µg/ml) in the medium without FBS for 24 h at 37°C. (b) The fluorescent images of macrophages revealing the calcium uptake. Macrophages were treated with the culture medium containing PU NPs (50 µg/ml) and Calcium Green-1 AM (200 nM) for 24 h. Scale bar represents 20 µm. (c) Quantitation of Calcium Green-1 AM positive cells by flow cytometry after incubation with PU NPs (50 µg/ml) and Calcium Green-1 AM (200 nM) for 24 h. * $p < 0.05$, among the indicated groups. (d) The ATR-FTIR spectra of PU NPs of PU3. “PU3-m” indicates the samples after incubation in DMEM medium for 24 h.

Fig. 5 (a) The LC3-II protein expression for macrophages treated with PU NPs (50 µg/ml) for 18 h. (b) The LC3-II protein expression for macrophages treated with PU3 (50 µg/ml) and LPS (100 ng/ml) for 24 h. GAPDH was used as the internal control. Band intensities were quantified and normalized to GAPDH. (c) Fluorescent images of LC3 for macrophages exposed to PU3 (50 µg/ml) and LPS (100 ng/ml) for 24 h. Scale bar represents 20 µm. (d) The mRNA expressions of autophagy-related genes for macrophages after incubation with PU3 (50 µg/ml) and LPS (100 ng/ml) for 24 h. (e) The viability of macrophages after treatment of LPS and PU3 for 24 h. * $p < 0.05$, among the indicated groups. ns, no significant difference.

Fig. 6 (a) The colocalization of LC3 (green) and p-NF- κ B (red) after incubation with PU3 (50 μ g/ml) and LPS (100 ng/ml) for 24 h. The colocalized vesicles appeared in yellow. Scale bar represents 20 μ m. (b) The p-NF- κ B protein expression for macrophages after the treatment of PU3 (50 μ g/ml) and LPS (100 ng/ml) for 24 h. (c) Inhibition of the NP-induced LC3-II protein expression in macrophages by the treatment of EGTA or Baf-A1. Macrophages were incubated with PU3 (50 μ g/ml) and LPS (100 ng/ml) for 24 h after the culture medium was mixed with EGTA (100 nM) or Baf-A1 (200 pM). GAPDH was used as the internal control. Band intensities were quantified and normalized to GAPDH. (d) The mRNA expressions of proinflammatory cytokines analyzed by qRT-PCR. $*p < 0.05$, among the indicated groups.

Fig. 7 (a) Representative pictures of NR labeling of macrophages at 3.5 dpf. (b) The mRNA expression of proinflammatory cytokines. (c) The survival rate of zebrafish embryos injected with LPS into the yolk at 3 dpf and subsequently monitored for 48 h. Embryos injected with H₂O served as the blank control. $*p < 0.05$, among the indicated groups. ns, no significant difference.

Fig. 8 Scheme of immune suppressive activities of PU NPs in macrophages. PU NPs adsorbed calcium through surface carboxyl groups and transported the calcium into macrophages. The increased intracellular calcium may enhance autophagy and reduce NF- κ B pathway via autophagy-lysosomal degradation. The *in vivo* zebrafish inflammation model supported the immunosuppressive activities of PU NPs to reduce the animal mortality by inhibiting the macrophage recruitment and proinflammatory responses. Hence, PU NPs exhibit surface COO^- dose-dependent immunosuppressive properties.

Table 1. The primer sequences used for qRT-PCR analyzes.

Gene	Primer sequences	Primer annealing temperature (°C)
IL-1β	F: GCTGCTTCCAAACCTTTGAC R: TTCTCCACAGCCACATGAG	62
IL-6	F: GGACCAAGACCATCCAATTC R: GGCATAACGCCTAGGTTTG	62
TNF-α	F: GCTTTCCGAATTCCTGGAG R: TTGCACCTCAGGGAAGAATC	62
Atg5	F: TAGAGCCAATGCTGGAAACC R: TGTTCCTCCACTGAACTTG	62
beclin 1	F: AGCAAAGAACCCTGCCATAG R: TGCCACAAGCATCTCATCTC	62
cathelicidin	F: AATTTTCTTGAACCGAAAGGGC R: TGTTCCTCAGATCCTTGGGAGC	62
Mtor	F: CCAGAAGGGTCTCCAAGGAC R: AGGCAGCATTGAAGAGATCC	62
GAPDH	F: GGCAAAGTGGAGATTGTTGC R: AATTTGCCGTGAGTGGAGTC	60
zf IL-1β	F: TGGACTTCGCAGCACAAAATG R: GTTCACTTCACGCTCTTGGATG	60
zf IL-6	F: AGACCGCTGCCTGTCTAAAA R: TTTGATGTCGTTACCAGGA	60
zf TNF-α	F: GCTGGATCTTCAAAGTCGGGTGTA R: TGTGAGTCTCAGCACACTTCCATC	60
zf GAPDH	F: ACCCGTGCTGCTTTCTTGAC R: GACCAGTTTGCCGCCTTCT	60

Table 2. The hydrodynamic diameter and zeta potential of various PU NPs prepared in the study.

Sample	Hydrodynamic diameter (nm)	Zeta potential (mV)
PU1	64.3±0.8	-48.1±2.9
PU2	41.9±0.7	-63.1±3.5
PU3	34.0±1.3	-70.8±0.8

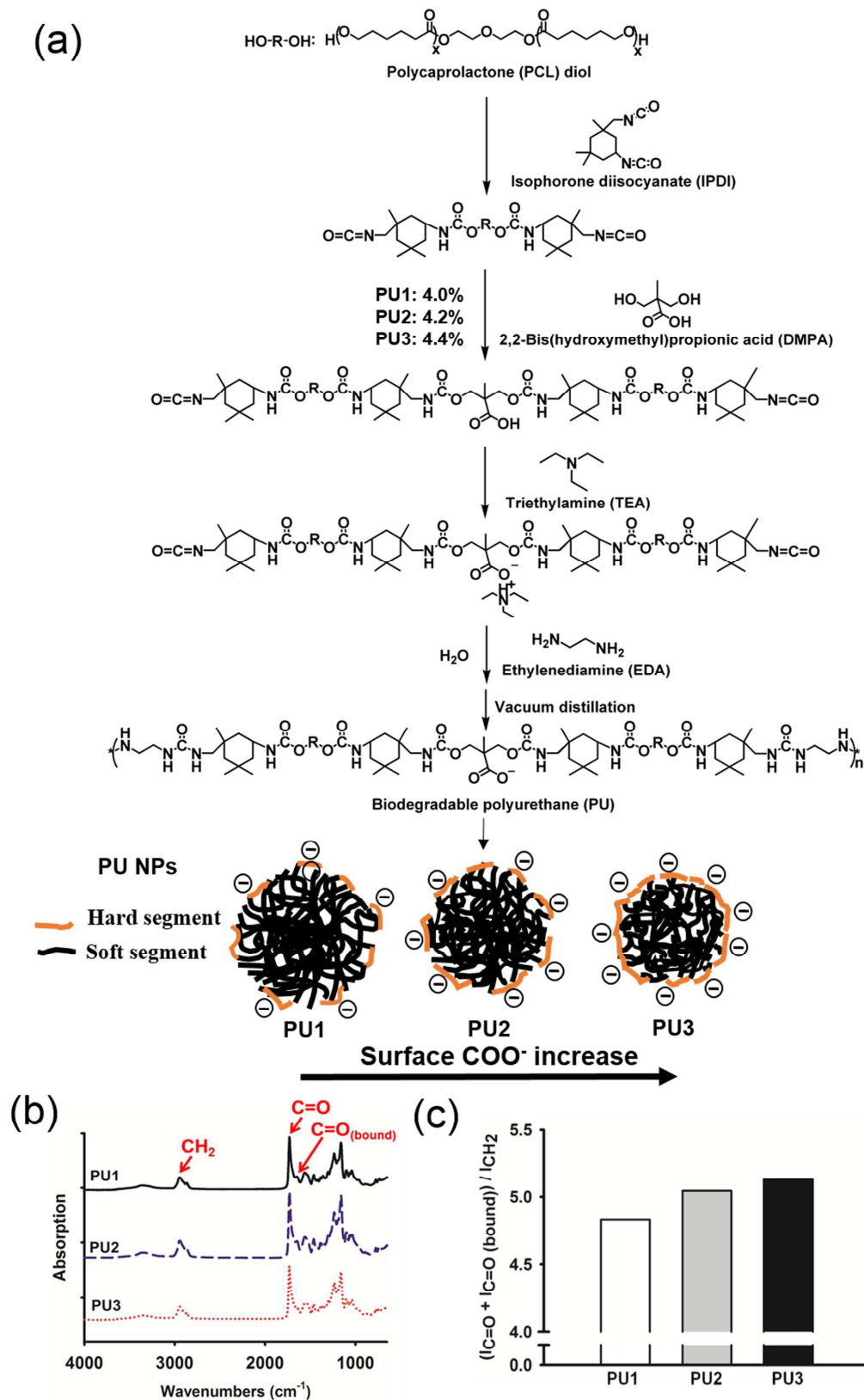


Figure 1

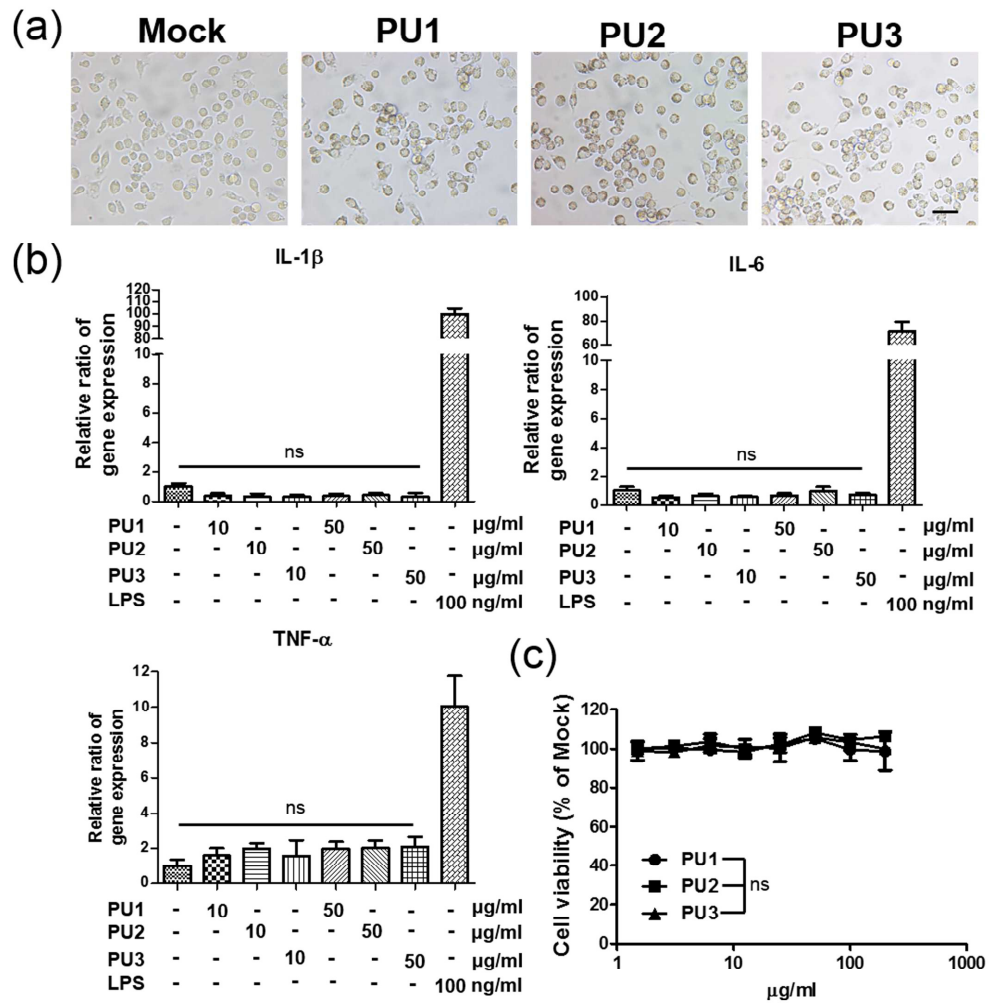


Figure 2

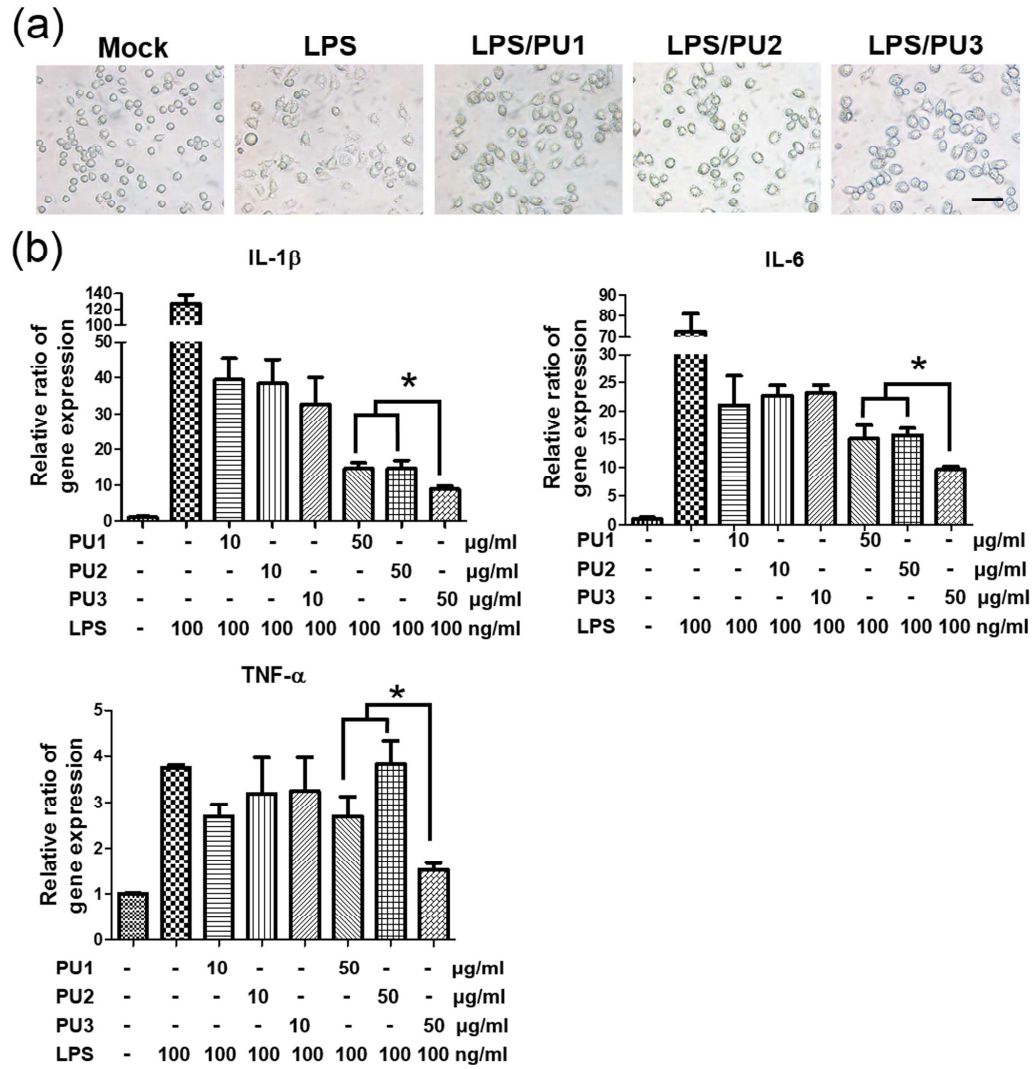


Figure 3

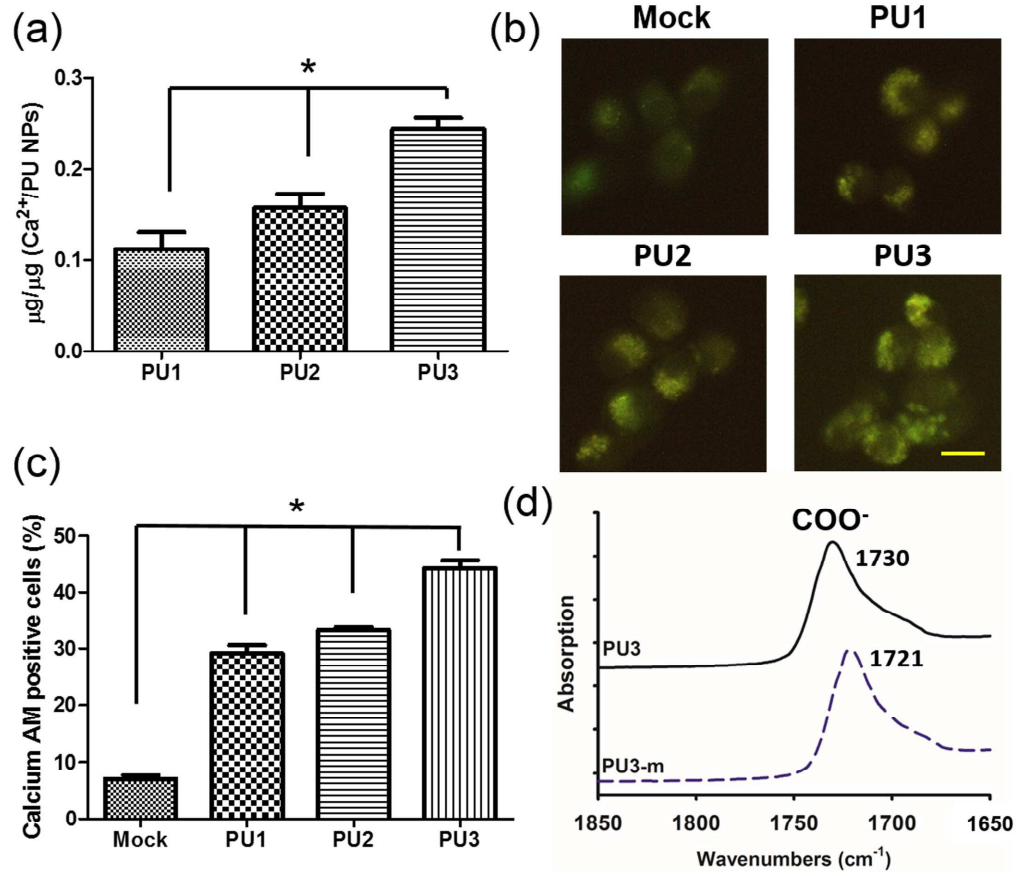


Figure 4

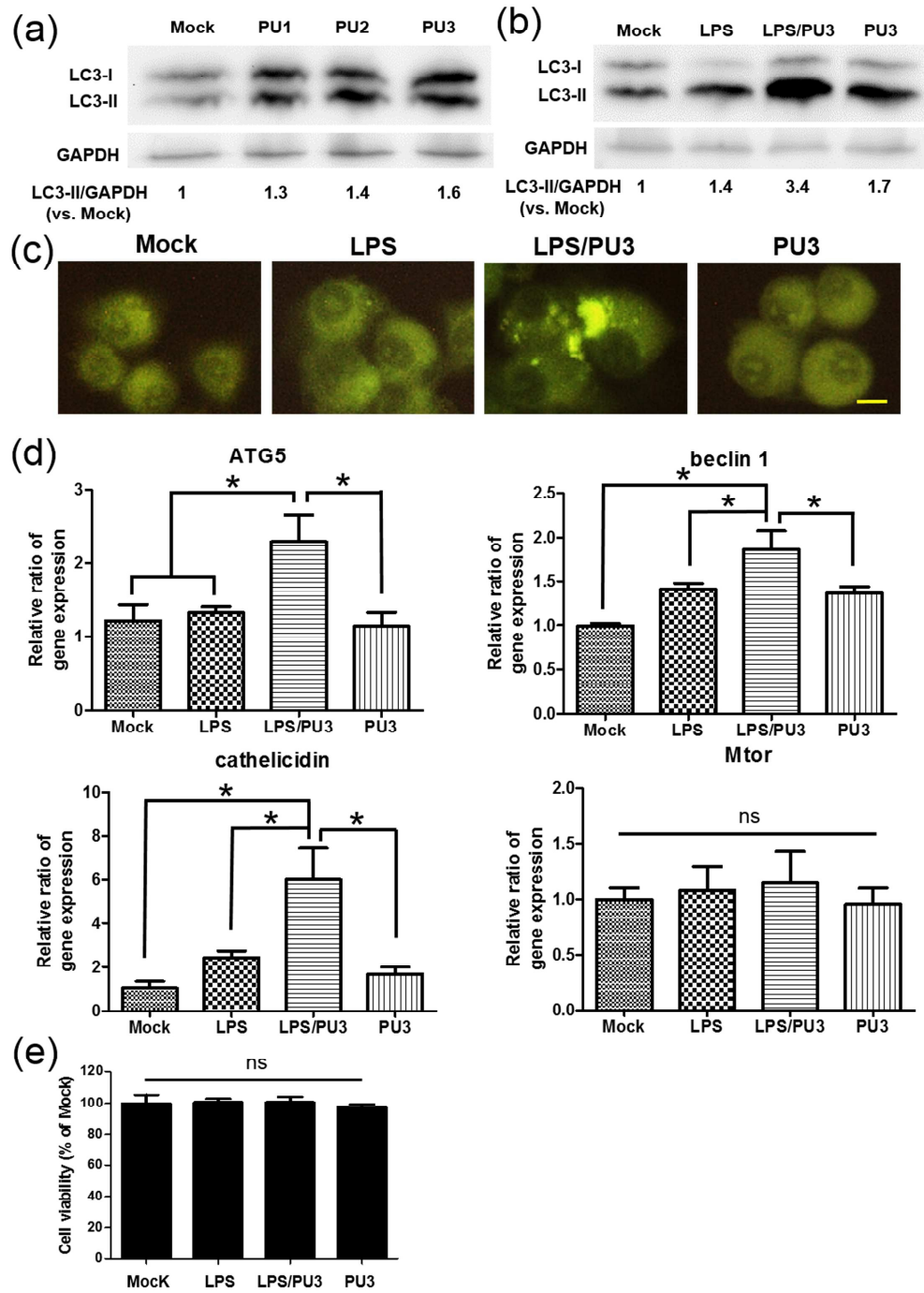


Figure 5

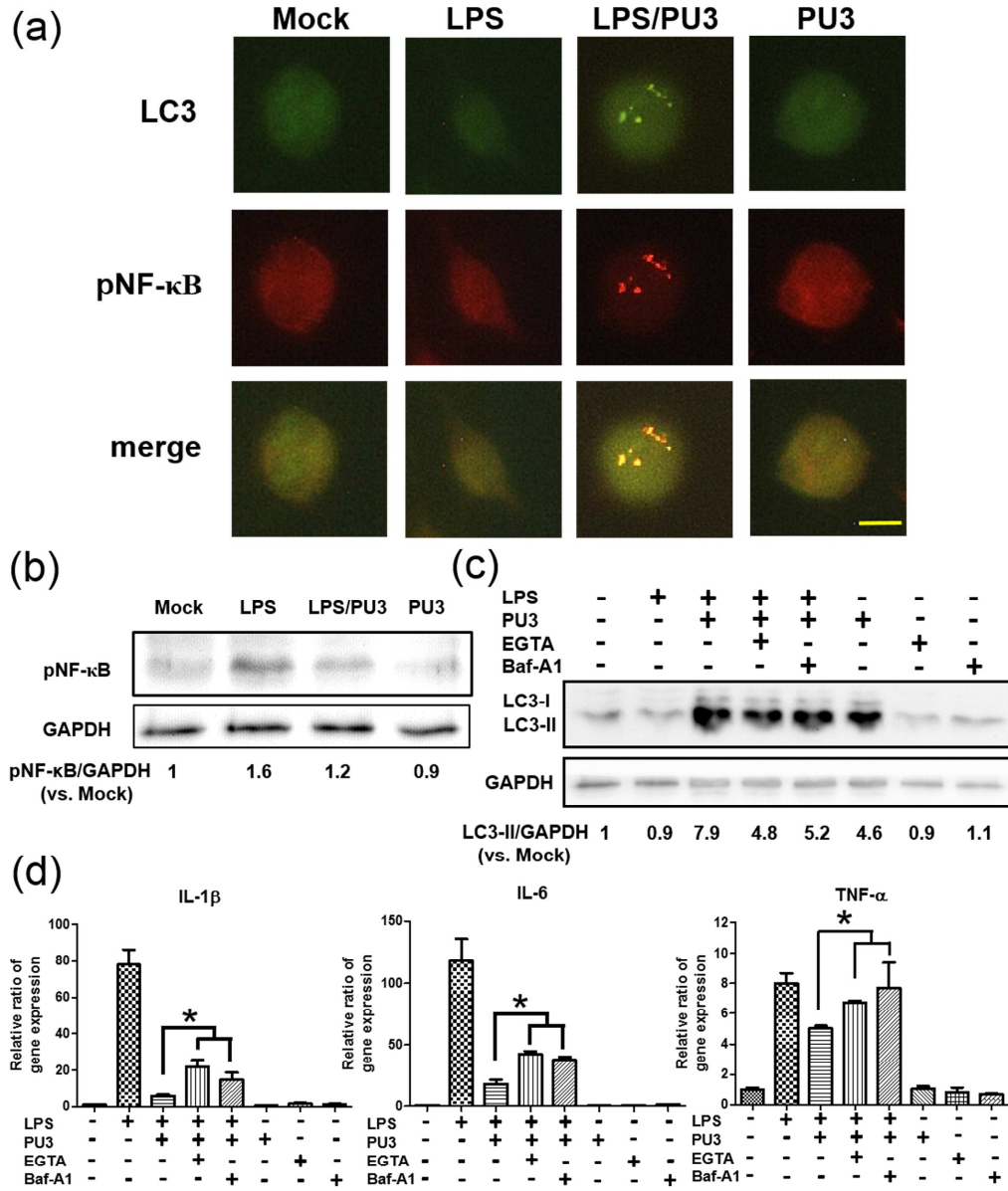


Figure 6

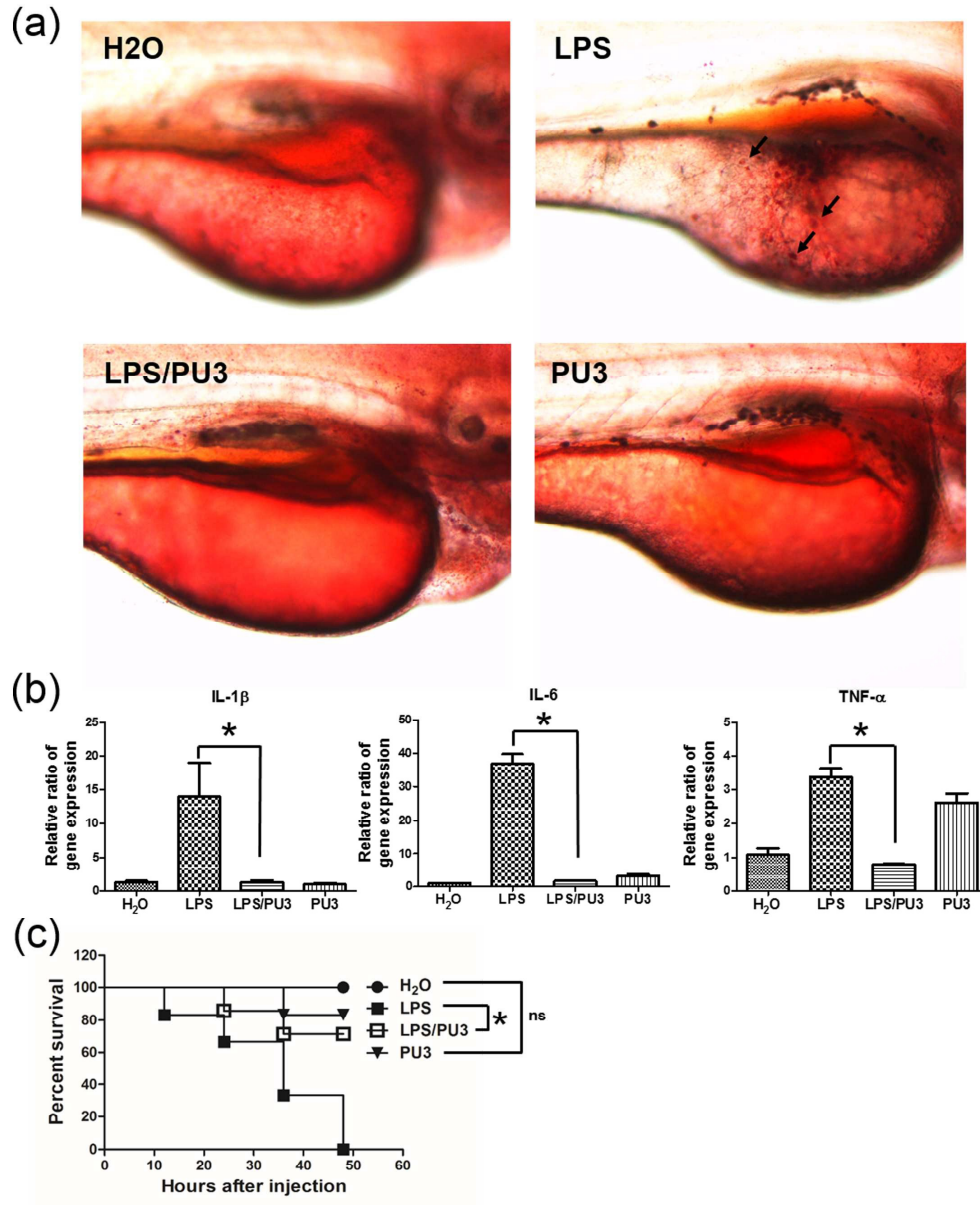


Figure 7

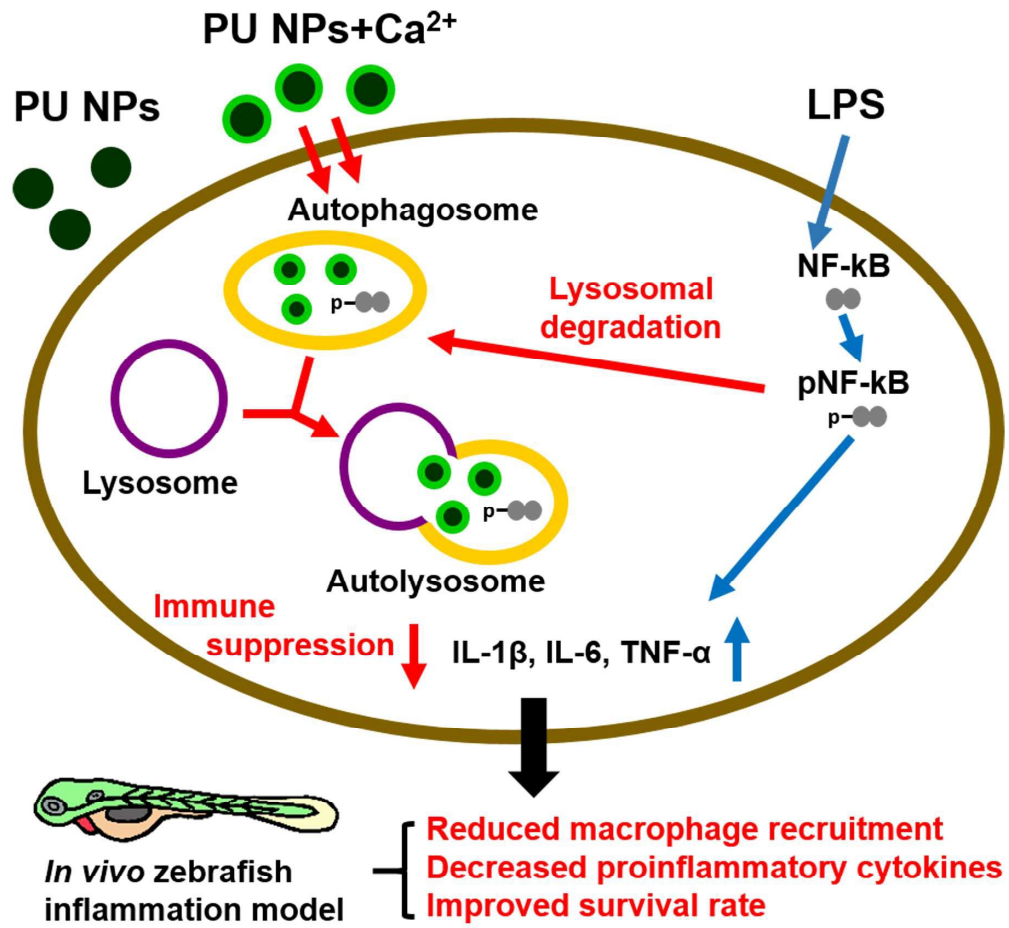


Figure 8